

Fig. 9. Measurements of $\arg(\Gamma_1) - \arg(\Gamma_2)$ versus frequency for two connections of a 10-cm air transmission line terminated in an open circuit.

predominantly at the current maxima. The measurements of $\arg(\Gamma_1) - \arg(\Gamma_2)$ are similar to those shown previously in that the changes occur at the current maxima.

IV. DISCUSSION

It should be emphasized that the purpose of this paper is to show that some of the measurement discrepancies observed because of connectors can be explained with a simple connector joint model. It is not meant to be an exhaustive study of connector joints. Much work remains to be done in both understanding and modeling connector joints. The intent of this paper is to document some of the current observations.

Much of the work to date reaffirms the complexity of the connector joint. Ideally, one would expect the resistive component to vary with frequency as $f^{1/2}$. However, as noted by Daywitt [1], variation of up to $f^{2.8}$ has been observed. The inductive term can also exhibit a complex behavior as a function of frequency. Fig. 9 shows one example of this complexity. Plotted here is $\arg(\Gamma_1) - \arg(\Gamma_2)$ for the 10-cm air transmission line terminated in an open circuit. Note that the sign of the phase change is negative at 8 GHz and positive at the lower frequencies. This type of behavior is not explainable with the simple model shown.

Also, it is not known what effect the network analyzer calibration errors have. Network analyzers, to some degree, can transform phase information into magnitude and magnitude into phase information. The extent to which this is happening is beyond the scope of this study. Numerous network analyzer calibrations were used in collecting the data for this report.

V. CONCLUSIONS

The simple connector joint model described in this paper appears to be a valuable tool in understanding the changes that occur at connector joints. Theory predicts that the changes in Γ due to changes in resistance or reactance can be up to four times greater for highly reflecting devices than for nonreflecting devices. These changes are frequency dependent and are greatest at or near the current maxima or the current nulls.

Measurements of $|\Gamma_1| - |\Gamma_2|$ are shown for two different connections of highly reflecting devices with 14-mm connectors. These measurements are used to estimate the changes in normalized joint resistance at the connector. Similarly, measurements of $\arg(\Gamma_1) - \arg(\Gamma_2)$ are shown for two different connections. These measurements are used to estimate the changes in normalized reactance. For the devices shown, the changes primarily occur at

the current maxima, which means the changes are in the resistance and inductive components of the connector joint.

ACKNOWLEDGMENT

The author is indebted to W. C. Daywitt for his numerous contributions in the development of this paper. The author would also like to acknowledge the efforts of R. L. Ehret and J. R. Yehle in collecting and preparing the data for this paper. Finally, the author would like to thank C. A. Hoer for his continued support in this effort.

REFERENCES

- [1] W. C. Daywitt, "A simple technique for investigating defects in coaxial connectors," pp. 460-464, this issue.

A Simple Technique for Investigating Defects in Coaxial Connectors

WILLIAM C. DAYWITT

Abstract—This paper describes a technique that uses swept-frequency automatic network analyzer (ANA) data for investigating electrical defects in coaxial connectors. The technique will be useful to connector and ANA manufacturers and to engineers interested in determining connector characteristics for error analyses. A simplified theory is presented and the technique is illustrated by applying it to perturbations caused by the center conductor gap in a 7-mm connector pair.

Key terms: ANA, coaxial connector, error analysis, stepped-frequency measurements.

I. INTRODUCTION

Most analyses underlying microwave measurement procedures assume ideal connectors at the various measurement ports, although it has been recognized for some time that errors due to this idealization would have to be accounted for sooner or later. With computerization and greater sensitivity and stability, modern systems are now at that point. For example, if a swept-frequency reflection measurement of an open circuit not used in the automatic network analyzer (ANA) calibration is performed, then the measured reflection coefficient magnitude often varies in a strongly oscillatory manner below and above unity magnitude, while the obvious result should be a magnitude that remains below unity and slowly diminishes monotonically with frequency. This type of result has been noted by a number of ANA users. Studies [1] have shown that the oscillatory phenomenon just described is due to connector loss at the joint in the connector pair where the center conductors from the two connectors comprising the pair meet, and also that the oscillations can be used to determine the magnitude of that loss even in the presence of considerable ANA error.

Recent investigations indicate that reactive defects at the same joint in the connector pair cause phase variations similar to the magnitude oscillations, and that the envelope of these variations can be used to determine the magnitude of the reactance responsible for the variations.

Manuscript received July 28, 1986; revised November 29, 1986.
The author is with the Electromagnetic Fields Division, National Bureau of Standards, Boulder, CO 80303.
IEEE Log Number 8613289.

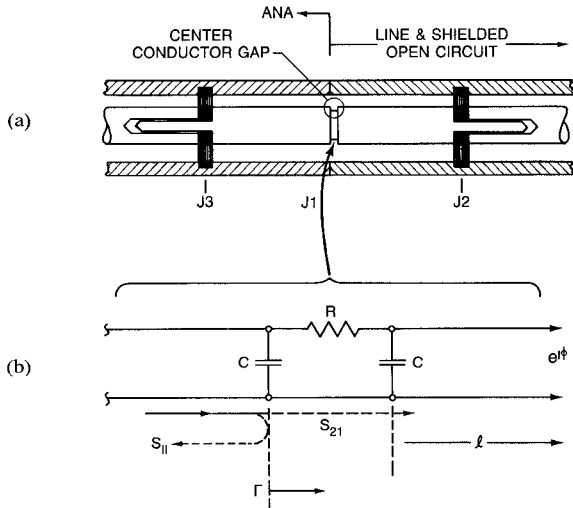


Fig. 1 (a) Longitudinal section of an air line and a shielded open circuit. (b) An equivalent circuit

A simple technique has evolved from these studies that appears to be useful for investigating connector defects. It consists of terminating the connector pair under investigation with a length of line ending in a shielded open circuit. The length is chosen to produce a rapidly varying phase difference between the incident and reflected fields at the connector as the frequency is varied. The resulting reflection coefficient (both magnitude and phase) when plotted as a function of frequency includes a rapidly varying component that contains information about the connector defects which can be easily determined from the plot.

This paper will develop a theory behind these observations and apply it to a simple model of the gap at the center conductor joint in a 7-mm connector pair through the use of computer simulations and ANA measurements.

II. THEORY

For illustrating the technique, it is convenient to model the connector pair in terms of the center conductor joint alone, ignoring smaller defects at the center conductor bead supports and at the outer conductor joint. The connector pair is shown in Fig. 1(a). An equivalent circuit of the center conductor joint J1 is shown in Fig. 1(b); it consists of two shunting capacitors and a series resistance. The normalized resistance r and the normalized admittance y of the joint are given by the equations

$$r = R/Z_0 \tag{1}$$

and

$$y = j\omega CZ_0 \tag{2}$$

where ω and Z_0 are the radian frequency and the characteristic line impedance, respectively. The normalized resistance r is assumed to vary as the square root of the frequency [1], [2], while C is assumed to be frequency insensitive [3]. It can be shown that the scattering parameters of the junction are related to these normalized quantities through the equations

$$S_{11} = S_{22} = r/2 - y \tag{3}$$

and

$$S_{21} = S_{12} = 1 - r/2 - y \tag{4}$$

to first order in r and y . The reflection coefficient Γ of the line

and junction is calculated from the formula

$$\Gamma = S_{11} + \frac{S_{12}S_{21}e^{-2\gamma l + j\phi}}{1 - S_{22}e^{-2\gamma l + j\phi}} \tag{5}$$

where γ and l are the propagation constant and the length of the line, and $e^{j\phi}$ is the reflection coefficient of the open circuit. The phase of the open circuit is ϕ . The equation that results from reducing (5) to first order in r and y is

$$\Gamma = e^{-2j\beta l + j\phi} \{ 1 - 2\alpha l - r[1 - \cos(2\beta l - \phi)] - 2y[1 + \cos(2\beta l - \phi)] \} \tag{6}$$

where α and β are the real and imaginary parts of γ . The magnitude and phase of Γ in (6) can be approximated by

$$|\Gamma| = 1 - 2\alpha l - r[1 - \cos(2\beta l - \phi)] \tag{7}$$

and

$$\theta \equiv \arg(\Gamma) = -2\beta l + \phi - 2|y|[1 + \cos(2\beta l - \phi)]. \tag{8}$$

The last term in (7) shows that the magnitude of Γ is affected by the normalized resistance r but not by the normalized admittance y . Similarly, the phase of Γ is affected by y but not by r . If the line length l is a number of wavelengths, the r and $|y|$ terms in (7) and (8) are rapidly varying and easily distinguished from the other terms in the equations when $|\Gamma|$ and θ are plotted as a function of frequency. It is this feature that permits the scattering coefficients of the joint to be easily determined from the reflection data.

The center conductor bead supports at J2 and J3 in Fig. 1(a) are assumed to be matched to the lines on both sides of the beads. The symbols J2 and J3 refer to the contact losses at these positions where the center conductors are rejoined after passing through the beads, generating the same type of normalized contact resistances discussed for joint J1. Additional comments about the model and about (7) and (8) are presented in the Appendix.

III. COMPUTER SIMULATIONS

The results of a computer simulation are employed in this section to illustrate how the oscillations caused by the resistance and capacitances in Fig. 1(b) are used to determine r and $|y|$ under ideal conditions. Values of $0.006f^{0.5}$ for r and 0.002 pF for C [3] are used in generating the simulated curves. The length of the line is 30 cm, and the attenuation constant α corresponds to a gold-plated 7-mm line. Equations (7) and (8) are plotted as a function of frequency with these values inserted. The computer-generated results are shown in Fig. 2(a) and (b). The oscillations in Fig. 2(a) are due to the J1 joint loss (i.e., the normalized resistance r), and (7) implies that the two envelope curves connecting the maxima and minima are separated by $2r$. Therefore, r is determined by plotting the measured reflection coefficient magnitude as a function of frequency, drawing in the envelope, and measuring the separation between the envelope curves.

The simulated phase oscillations are shown in Fig. 2(b) with the first two terms in (8) removed. The last term in (8) implies that the envelope separation in the figure is equal to $4|y|$, showing how to determine $|y|$ (and hence C via (2)) from the measured phase data.

No ANA error is included in the model leading to Fig. 2(a) and (b), so they represent an idealization of what is to be expected in an actual measurement. It is assumed in using the technique that the ANA characterization error is slowly varying,

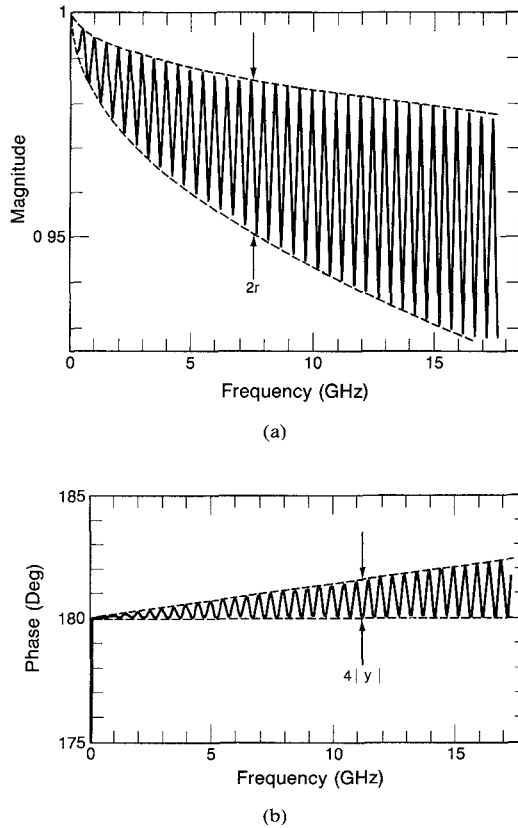


Fig. 2. (a) Computer simulation of the magnitude of the reflection coefficient Γ for $r = 0.006f^{0.5}$. (b) Computer simulation of the phase of the reflection coefficient Γ for $C = 0.002$ pF.

in which case the ANA error tends to cancel out since measurement data differences are used in calculating the envelope widths in Fig. 2(a) and (b).

IV. MEASUREMENTS

In order to create a single joint J1 and avoid the complication of including J2 in the measurement (see Fig. 1(a)), a 30-cm air line was connected to the ANA with the free end of its center conductor supported by a dielectric bead. A short length of outer conductor was connected to the free end of the air line outer conductor to form a shielded open circuit. The magnitude and the phase of the reflection coefficient of the combination were then measured and plotted as a function of frequency, the results of which are shown in Fig. 3(a) and (b). Fig. 3(a) shows the magnitude of the reflection coefficient as the frequency varies from 0.045 to 18 GHz along the abscissa. The ordinate is the reflection coefficient, and the scale varies from 0.84 at the bottom of the plot to unity in 0.02 steps. The oscillations in the graph are similar to those of Fig. 2(a) except that the averages of the two curves do not track, possibly because of ANA error. The width of the envelope was calculated at the frequencies shown in the figure and the separation is given by $2r$ (see Fig. 2(a)), where r can be expressed as

$$r = C_1 f^{1/2} \quad (9)$$

since it is assumed to vary as the square root of the frequency. When (9) is fit to the data in the figure, C_1 is found to be 0.012 per square root frequency.

Fig. 3(b) shows the phase of the reflection (including an electrical delay of 2 ns) as a function of frequency. The delay is

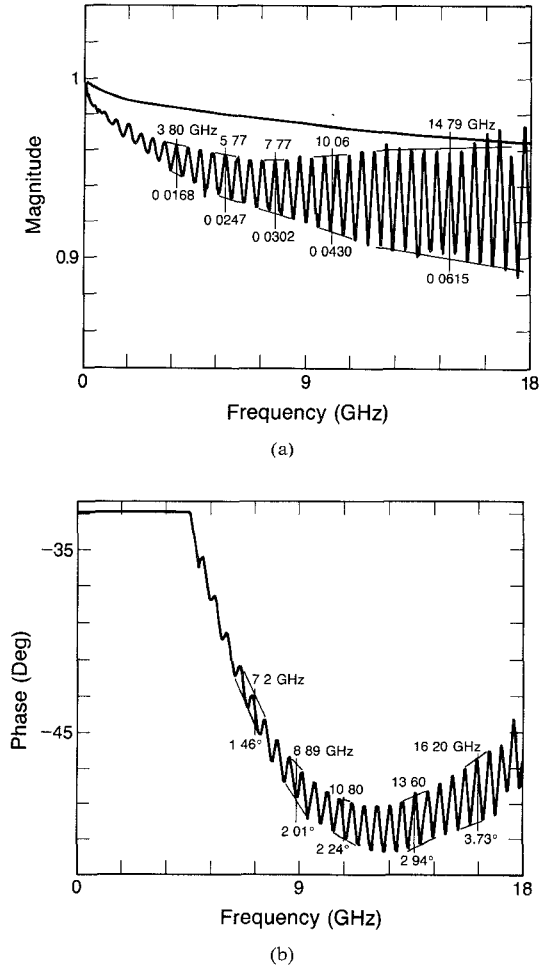


Fig. 3. (a) Measured reflection coefficient magnitude of a 7-mm connector line terminated in a shielded open circuit. (b) Measured reflection coefficient phase of a 7-mm connector line terminated in a shielded open circuit.

included to suppress the steep negative ramp (corresponding to the first two terms in (8)) characteristic of such data, enabling the oscillations to be more easily discerned. Equation (2) implies that $|y|$ can be expressed in the form

$$|y| = C_2 f. \quad (10)$$

Applying (10) and the fact that the envelope separation is given by $4|y|$ (Fig. 2b) to the data in Fig. 3(b) results in a C_2 of 0.00074 rad/GHz.

The scattering parameters of the joint may now be calculated from C_1 , C_2 , and (3) and (4):

$$S_{11} = S_{22} = 0.017f^{1/2}/2 - j0.00074f \quad (11)$$

and

$$S_{21} = S_{12} = 1 - 0.017f^{1/2}/2 - j0.00074f. \quad (12)$$

The corresponding lumped circuit parameters of Fig. 1(b) may be determined through (1) and (2), if desired.

V. DISCUSSION

The measurement technique is still in its formative stages and the description just presented glosses over a number of finer points that require comment.

The first comment concerns how to combine the other defects within a connector pair to obtain a complete description of the pair as a microwave junction, and how to measure these other

defects. In the present context, a joint is defined as a discontinuity whose longitudinal extension is small compared to a wavelength. J1 through J3 in Fig. 1(a) are examples, where J1 is the joint considered in the previous sections, and J2 and J3 are at the center conductor bead supports. The joints are far enough apart so that no sizeable overlapping between the higher order mode fields generated by these defects takes place. Thus, reflections from these joints may be combined by using standard transmission-line equations [4] to obtain the complete scattering description of the connector pair.

The procedure described in the previous sections is concerned with the measurement of joint J1 in Fig. 1(a) without J2 being present and with joint J3 included as part of the ANA calibration. The question of measuring J1 and J2 simultaneously has been partially answered in an earlier paper [1], which involved the determination of the losses (i.e., the r 's) of these two joints simultaneously. Inclusion of the reactive components (the y 's) in the theory has not as yet been completed, but does not appear to present a serious problem.

The second comment relates to the general validity of the technique. Starting from an arbitrary tee or pi network and reducing the results to first order, it can be shown that the joint scattering parameters take the form

$$S_{11} = S_{22} = z/2 - y \quad (13)$$

and

$$S_{21} = S_{12} = 1 - z/2 - y \quad (14)$$

where z and y are complex numbers with positive real parts, and where z has the form of a normalized impedance and y that of a normalized admittance. The equations show that the first-order joint defined by this process is both reciprocal and symmetric. The volumetric RF loss of most commercial beads is small because the bead width is small and the loss tangent of the bead material is also small. Furthermore, there is no physical evidence to suggest an inductive shunting element between the conductors for the type of joints encountered in a connector. Therefore, y can be assumed to be positive and purely imaginary. On the other hand, the most that can be said about z is that its imaginary part is positive since there is no reason to assume a significant series capacitive element (see the Appendix) in any of the joints. It is convenient to summarize these observations in the following equations:

$$z = r + ja \quad (15)$$

and

$$y = jb \quad (16)$$

where a and b are positive real numbers. By repeating the steps leading to (7) and (8), it is possible to show that

$$\theta = -2\beta l + \phi - a[1 - \cos(2\beta l - \phi)] - 2b[1 + \cos(2\beta l - \phi)]. \quad (17)$$

$|\Gamma|$ is the same as in (7) and shows that the joint loss can be determined as before [1]. Equation (17), however, contains the inductive component ja of z that combines with the capacitive component jb of y . These components are easily separated, however [5].

The third and final comment concerns how the envelopes in Figs. 2 and 3 open up. The vertical separation between the envelopes in Fig. 2(a) was assumed to increase as the square root of the frequency and represents what would happen for the theoretical, ideal joint. However, a closer examination of Fig. 3(a)

shows that the envelope opens up at a rate that is linear in the frequency, implying that the insertion loss of the connector joint J1 increases more rapidly than $f^{0.5}$. This is contrary to what is generally thought. A number of other experiments show patterns where the loss of J1 varies from the square root of the frequency to a rate as high as $f^{2.8}$, and even more pathological behaviors. It is the opinion of the author that this anomalous behavior is real, and that it is due to interactions taking place inside the center conductor joint J1 when the center conductors do not mate squarely. More will be said concerning this phenomenon in a subsequent paper.

Figs. 2(b) and 3(b) are in good agreement with the theoretical rate of separation of their respective envelopes.

VI. CONCLUSIONS

A simple technique has been presented that will aid investigations of coaxial connectors and provide a better understanding of the mechanisms responsible for their nonideal behavior. Although the theory presented here applies to the simple type of gap depicted in Fig. 1, there is reason to believe that the theory and technique can be expanded to provide a powerful tool for examining connector defects in general. This conclusion is supported by a growing body of experimental evidence. Connector repeatability measurements using this technique have already begun to bear fruit [5].

APPENDIX

Model

The discussion in Sections I–IV concerning the electrical effects of the gap constituting joint J1 was simplified in order to concentrate on the technique under investigation. A more realistic look at this joint is provided in Fig. 4(a), where the gap width is Δl . The magnitude of the total current across the gap at radius a is close to I (the conduction current on the center conductor away from the gap) since the gap width is small and the magnetic field at this radius is approximation H_0 . This total current breaks down into a displacement component I' and a conduction component I'' in the gap. The fields in the gap can be approximated by a TEM radial waveguide mode [6] since the small width Δl prevents the higher order TM modes from penetrating a significant distance into the gap.

Fig. 4(b) shows an equivalent circuit for the gap and two approximations [7] that can be used to obtain an order-of-magnitude estimate of the circuit parameters C' and L . The parameters already discussed in conjunction with Fig. 1(b) are shown as dashed symbols and will be ignored in the following discussion. When the TEM mode fields are inserted into the equations appearing in the figure, the capacitive reactance (C') turns out to be at least five orders of magnitude larger than the inductive reactance. Therefore, the capacitance in Fig. 4(b) can be discarded, leading to the equivalent circuit in Fig. 4(c). The inductance is expressed in nH, where f is in GHz and Δl is in cm. The reflection coefficient S_{11} corresponding to this discontinuity is also shown in the figure. S_{11} is 0.012 for a maximum frequency and gap width of 18 GHz and 0.018 cm (0.007 in), respectively.

Technique

The standing wave set up on the line by the open circuit has the effect of alternately turning the resistance and the capacitors in Fig. 1(b) on and off as the frequency is varied. When the frequency is such that $\cos(2\beta l + \phi)$ is equal to +1, the total electric field E_r at the gap (Fig. 5(a)) is twice the incident field

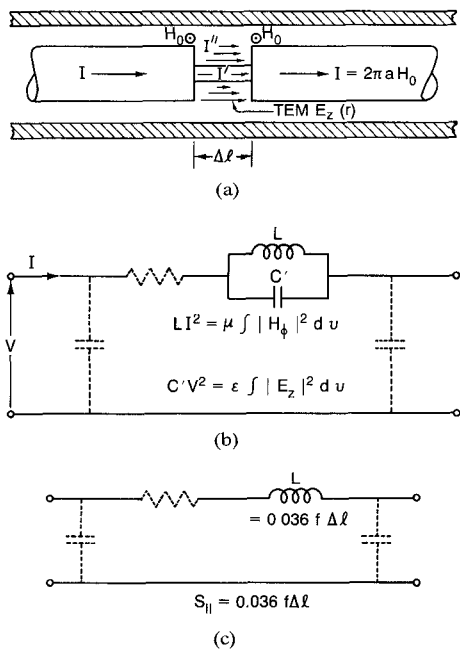


Fig. 4. (a) A close look at the fields and currents in the gap of joint J1. (b) An equivalent circuit for (a). (c) The inductance L and reflection coefficient S_{11} for J1.

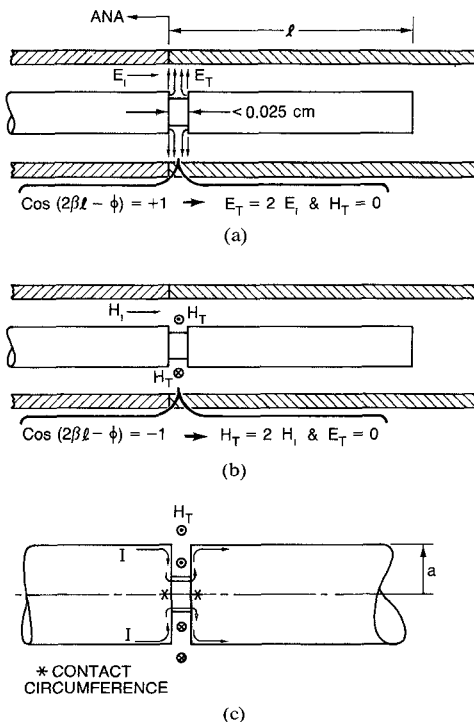


Fig. 5. (a) Longitudinal view of the line and open circuit where the frequency is such that the total electric field at the gap is a maximum and the magnetic field vanishes. (b) Longitudinal view where the frequency is such that the total magnetic field at the gap is a maximum and the electric field vanishes. (c) A closer view of the gap.

E_z , and the magnetic field vanishes. The gap is so narrow that no higher order modes penetrate it to reach the bottom of the gap, but their presence in the vicinity of the gap causes the fringing field shown in Fig. 1(b) and results in the discontinuity capacitances (last term in (8)). There is no current to penetrate the gap, so the gap resistance causes no voltage drop and goes unnoticed.

When the frequency is such that $\cos(2\beta l + \phi)$ is equal to -1 , the total magnetic field is twice the incident field, and the electric field vanishes (Fig. 5(b)). Now there are no electric field lines at all and the discontinuity capacitances are unexcited. However, the circulating magnetic field H_T (Fig. 5(c)) causes a current that samples the gap resistance r (last term in (7)). The current encounters the two contact resistances at the bottom of the gap that represent the metal-to-metal contacts in the actual connector joint. Current flowing across these contacts causes a significant loss, which is reflected in the normalized resistance r . The distributed or skin loss on the sides of the gap can also be included in r , although it is not significant compared to the contact loss.

ACKNOWLEDGMENT

The author is greatly indebted to four colleagues in the Electromagnetic Fields Division of the National Bureau of Standards: G. J. Counas, R. L. Ehret, J. R. Juroshek, and B. C. Yates.

REFERENCES

- [1] W. C. Daywitt, "A simple technique for determining joint losses on a coaxial line from swept-frequency reflection data," (to be published in) Proc. IEEE CPMT'86 Conf., Gaithersburg, MD, June 1986.
- [2] J. D. Jackson, *Classical Electrodynamics*. New York: Wiley, 1962.
- [3] J. R. Whinnery, H. W. Jamieson, and T. E. Robbins, "Coaxial-line discontinuities," *Proc. IRE*, p. 695, Nov. 1944.
- [4] D. M. Kerns and R. W. Beatty, *Basic Theory of Waveguide Junctions and Introductory Microwave Network Analysis*. New York: Pergamon Press, 1967.
- [5] J. R. Juroshek, "A study of measurements of connector repeatability using highly reflecting loads," pp. 457-460, this issue.
- [6] N. Marcuvitz, ed., *Waveguide Handbook*. New York: McGraw-Hill, 1951.
- [7] R. E. Collin, *Foundations for Microwave Engineering*. New York: McGraw-Hill, 1966.

Analysis of Waveguiding Structures Employing Surface Magnetoplasmons by the Finite-Element Method

NADER MOHSENIAN, MEMBER, IEEE, TERRY J. DELPH, AND DONALD M. BOLLE, FELLOW, IEEE

Abstract—The dispersion relation and electromagnetic field distributions for a gyroelectrically loaded waveguiding structure are obtained utilizing finite-element techniques. The structure considered consists of two layers, one a dielectric and the other a semiconductor, bounded by two perfectly conducting planes. The finite-element solution for the lowest real branches in the dispersion spectrum was compared against a numerical solution of the exact dispersion equation, and excellent agreement was found between the two. The structure, exhibiting nonreciprocal behavior, provides a suitable canonical model for the design of circuit components such as circulators, isolators, and phase shifters.

I. INTRODUCTION

The use of surface magnetoplasmons on semiconductor substrates shows promise in the development of components that can substitute for ferrite devices in the millimeter- and submillimeter-wave ranges [1]-[3]. Analytical studies of canonical struc-

Manuscript received August 18, 1986; revised November 28, 1986. This work was supported in part by the Army Research Office under Grant DAAG29-85-K-0081.

N. Mohsenian and D. M. Bolle are with the Department of Computer Science and Electrical Engineering, Lehigh University, Bethlehem, PA 18015.

T. J. Delph is with the Department of Mechanical Engineering and Mechanics, Lehigh University, Bethlehem, PA 18015.

IEEE Log Number 8612947.